Supporting Information

Understanding the charge transfer dynamics in 3D-1D nanocomposites over solar driven synergistic selective valorization of lignocellulosic biomass: A new sustainable approach

Arpna Jaryal,[a] Ajit Kumar Singh,[b] Shivali Dhingra,[a] Himanshu Bhatt,[a] Manvi Sachdeva,[a] Hirendra N. Ghosh,*[c] Arindam Indra,*[b] and Kamalakannan Kailasam*[a]

[a] Dr. Kamalakannan Kailasam
Advanced Functional Nanomaterials group,
Institute of Nano Science and Technology (INST),
Knowledge City, Sector 81, SAS Nagar, Manauli PO, Mohali, 140306, Punjab, India.
E-mail: kamal@inst.ac.in, kkamal17@gmail.com
[b] Dr. Arindam Indra
Department of Chemistry
Indian Institute of Technology (BHU)
Varanasi, 221005, Uttar Pradesh, India
E-mail: arindam.chy@iitbhu.ac.in
[c] Dr. Hirendra N. Ghosh
School of Chemical Sciences,
National Institute of Science Education and Research (NISER),
Bhubaneswar, 752050, Odisha, India
E-mail: hnghosh@niser.ac.in

EXPERIMENTAL SECTION

Materials and Reagents

Cadmium nitrate hexahydrate (SRL, India, extra pure), thiourea (Merck, India), ethylenediamine (SRL, India), aeroxide P25 TiO_2 nanoparticles (Sigma India, >99% purity) and absolute ethanol (Merck, India) were purchased and used without further purification.

Synthesis of CdS Nanorods

The CdS nanostructures were synthesized according to previously reported literature.[1] Briefly 3.11 mmol of $Cd(NO_3)_2.6H_2O$ and 9.32 mmol of thiourea were dissolved in 15 mL ethylenediamine separately and marked as solution A and B, respectively. Solution B was added into solution A and stirred for 15 min. The final mixture was then transferred into a Teflon lined autoclave and heated in an oven at 180 °C for 24 h. After cooling the reaction to room temperature, orange colored solid was collected by centrifugation (8000 rpm for 5 min). The collected product was washed with distilled water followed by ethanol and hexane. The final solid was then dried in a hot-air oven at 80 °C for 12 h.

Synthesis of TiO_2-CdS nanocomposite

The heterostructures of negatively charged CdS and positively charged TiO_2 with zeta potential values -19.9 mV [2] and +4.2 mV [3], respectively were successfully accomplished by the existing electrostatic interactions. Briefly certain amount of orange colored CdS powder and white colored TiO_2 powder were dispersed in ethanol separately. The uniformly dispersed TiO_2 solution was added into CdS solution and stirred for 24 h. The final self-assembled nanocomposite was collected by centrifugation and dried in vacuum-oven at 60 °C overnight.

Characterization Techniques

Powder X-ray diffraction (PXRD) patterns were recorded by Bruker D8 Advanced diffractometer equipped with a scintillation counter detector, with Cu-K_α radiation (λ = 0.15418 nm, 2θ = 5-80 °) source operating at 40 kV and 40 mA. PXRD pattern measurements confirmed the hexagonal phase of CdS (JCPDS #41-1049) with (hkl) planes (100), (002), (101), (102), (110), (103), (112) and (201) at 2θ values 25°, 26.7°, 28.3°, 36.8°, 43.9°, 48°, 52° and 52.9°, respectively. The

presence of anatase and rutile phase in P25 TiO_2 were also confirmed with prominent (hkl) planes (101), (004), (200), (105), (211), (204) and (116) at 25.2□, 37.7□, 47.9□, 53.8□, 55□, 62.6□ and 68.8□, respectively corresponds to anatase phase (JCPDS #21-1272) whereas planes (110), (101) at 27.3□, 36□ belongs to rutile phase (JCPDS #21-1276). X-ray photoelectron spectroscopy (XPS) study was performed with Al K_α X-ray source and a monochromator with ultra-high vacuum supplied by Thermo Fisher Scientific. The overall morphologies of nanostructures were observed with field emission scanning electron microscopy (FESEM, JEOL), the intimate contact of 1D CdS nanorods and 3D TiO_2 nanoparticles and lattice fringes were visualized with transmission electron microscope (TEM, JEOL) and high-resolution TEM (HRTEM), respectively. The acceleration voltage of TEM and HRTEM was set at 200 kV. Solid-state absorption spectra were recorded with Agilent Cary 100 UV-Vis spectrophotometer. Cyclic voltammetry curves and Nyquist plots were recorded using standard three-electrode cell setup with catalyst as working electrode, platinum wire as counter electrode, and Ag/AgCl as reference electrode in Metrohm Autolab workstation. For electrochemical studies, 0.1 M Na_2SO_4 aqueous solution was used as the electrolyte. The working electrode was prepared by coating slurry of photocatalyst on glassy carbon electrode (d = 0.2 cm) and drying overnight at room temperature. The photoluminescence emission (PL) spectra and time-resolved decay curves were recorded using Fluorolog 3−221 fluorimeter equipped with 450 W xenon lamp and LED laser, respectively. Gas Chromatography (GC) equipped with thermal conductivity detector (TCD) estimated the gaseous product (H_2) and GC equipped with mass spectroscopy (GC-MS) was used to quantify the liquid products, both provided by Shimadzu.

Ultrafast Transient absorption spectroscopy

A Ti: Sapphire-based femtosecond pump−probe LASER system (Astrella and Coherent) with a 35-fs pulse width at 1 kHz repetition rate wavelength centered at 800 nm was used to generate pump and probe pulse. A major part of the 800 nm laser beam (90%) was used to generate pump pulse which was passed through a non-collinear parametric amplifier (OPA) (OPerA-SOLO, model no. TO8U6WS). The pump beam from OPA is then sent to the Helios Fire transient absorption spectrometer where it is chopped at 500 Hz frequency for pump−probe experiments. The 800 nm monochromatic probe light was converted into visible region probe pulses by passing it through CaF_2. A delay line is employed in the spectrometer to create a delay between the pump and probe pulse. The samples were kept in a 2 mm cuvette, and the sample solutions were circulated to avoid sample degradation during the performance of the experiments. The optical density (OD) of the samples and pump fluence were kept same in order to maintain similar conditions. Surface Xplorer software was used to analyse the data, and the kinetic traces were achieved from time-resolved spectral data at appropriate wavelengths.

Photocatalytic Activity Measurements

The photocatalytic reactions were carried out in a home-made reactor vessel. In a typical reaction setup, certain amount of photocatalyst was dispersed uniformly in acetonitrile (ACN) solvent along with 50 mM HMF and 250 mM VanOL. The reaction mixture was then purged with argon gas to maintain inert atmosphere and was sealed properly. A 400 W xenon lamp equipped with 420 nm cut-off filter was used as visible light source. After performing the photocatalytic reactions at room temperature (25 °C) for certain time periods, gas samples were collected in gas-tight syringe and analyzed in GC. Further catalyst separation from solution was done by centrifugation and the collected liquid products were analyzed by GC-MS equipped with stable wax column. For conversion and yield measurements, calibration curves were drawn from known concentrations of samples injected in GC and GC-MS.

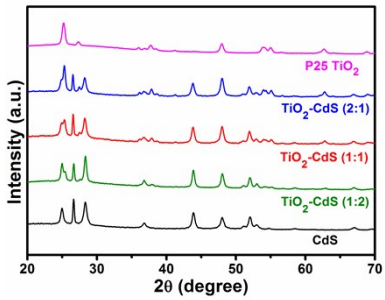

Figure S1. PXRD patterns of bare CdS, bare P25 TiO_2 and TiO_2-CdS heterostructures with (2:1), (1:1), and (1:2) weight ratios of P25 TiO_2 and CdS.

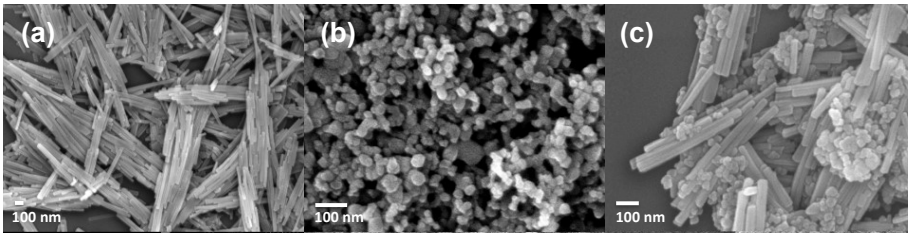

Figure S2. FESEM images of a) CdS nanorods, b) P25 TiO_2 particles, and c) TiO_2-CdS heterostructure.

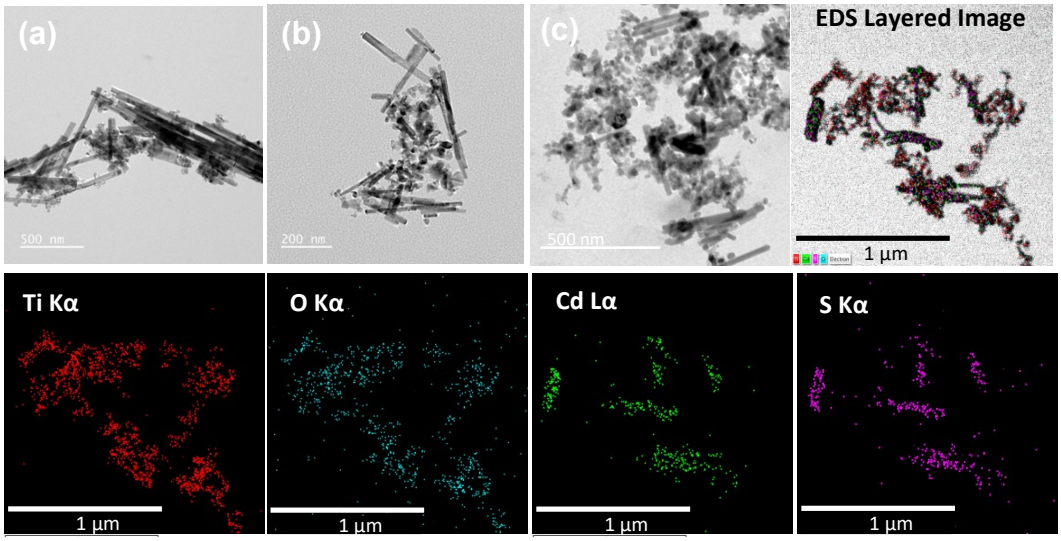

Figure S3. TEM Images (a-c) and Selected area EDX mapping of TiO_2-CdS with elemental mapping images of Ti, O, Cd, and S.

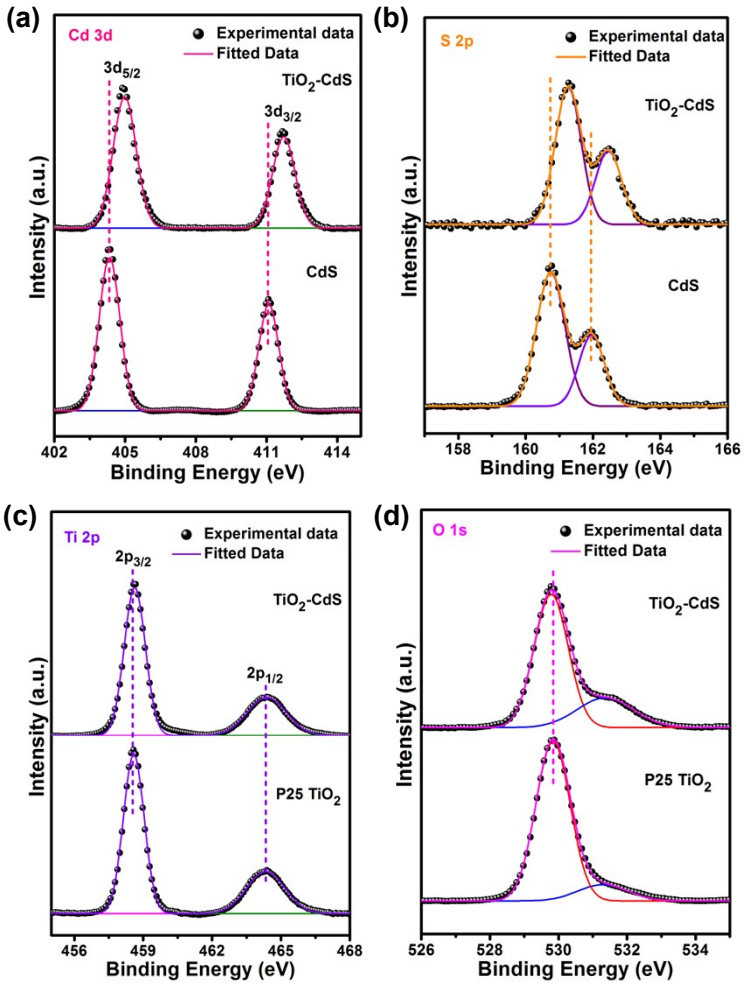

Figure S4. XPS high-resolution spectra of CdS, TiO_2 and TiO_2-CdS with elements a) Cd 3d, b) S 2p, c) Ti 2p and d) O 1s, respectively.

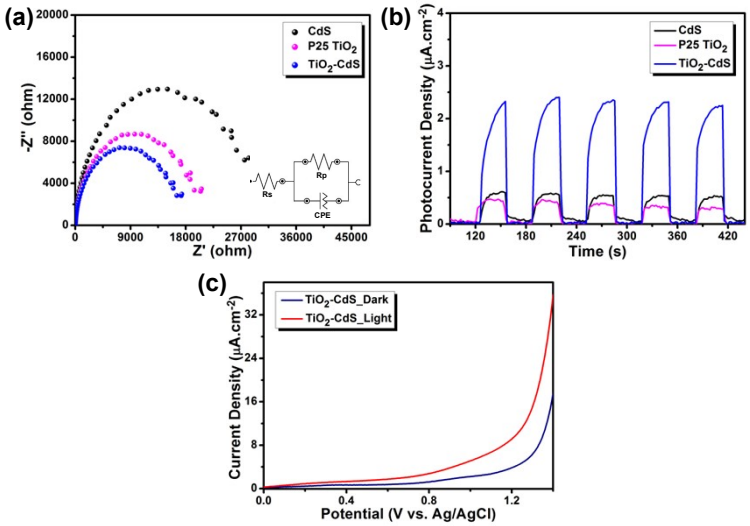

Figure S5. a) Electrochemical impedance spectroscopy (EIS) Nyquist plots of CdS, TiO_2 and TiO_2-CdS (inset- fitted Randles Circuit); b) Photocurrent density CdS, TiO_2 and TiO_2-CdS; and c) LSV of TiO_2-CdS under dark vs. under light.

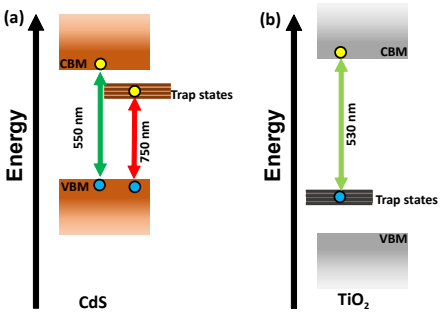

Figure S6. Schematic representation of the origin of the PL in (a) CdS nanorods and (b) P25 TiO_2, after the photoexcitation of 440 nm.

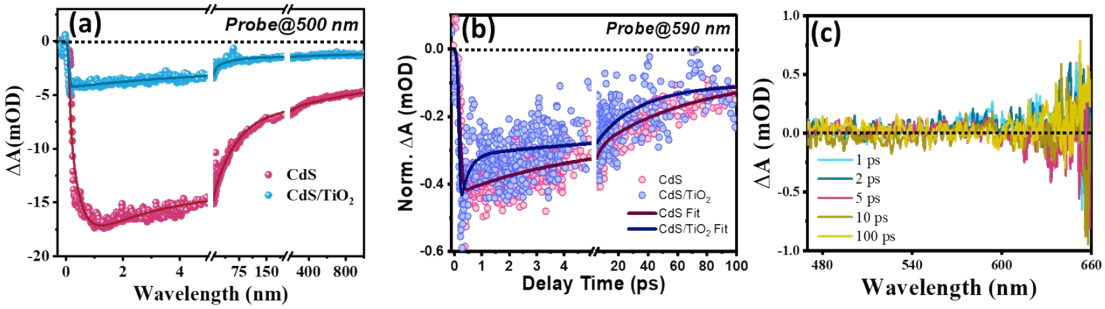

Figure S7. Comparative TA kinetics of CdS and TiO_2-CdS probed at 500 nm. (b) Normalised TA kinetics of CdS and TiO_2-CdS, monitored at trap state bleach position (590 nm) and (c) Transient absorption (TA) spectra of P25 TiO_2 at different pump-probe time delays after the photoexcitation of 440 nm.

Calculation of hot and band edge electron transfer rate in TiO_2-CdS heterostructure:

The rate constant k_{th} ($k_{cooling/thermalisation}$) corresponding to the hot carrier cooling processes for 1Σ in CdS nanorods can be calculated as

$$K_{th} = 1/\tau_{growth}$$

For τ_{growth} = 0.30 ps, k_{th} was calculated as 3.23 ps^{-1}.

For TiO_2-CdS heterostructure, the growth time scale of the 1Σ excitonic bleach signal was found to be 0.1 ps. This growth time in heterostructure can be written as following;

$$\tau_{growth,}\,(CdS/TiO_2) = 1/\,(k_{th} + k_{HET})$$

k_{hot} was calculated as 6.67 ps^{-1}. Hence, Hot electron transfer time; $\tau_{HET} = 1/k_{HET}$ was found as 0.15 ps.

Similarly the band edge electron transfer rate in TiO_2-CdS heterostructure (HS) was calculated using the following formula;

$$k_{BET} = (\tau_{d1,HS})^{-1} - (\tau_{d1,CdS})^{-1}$$

From the Table S2, $\tau_{d1,\ HS}$ = 1 ps and $\tau_{d1,\ CdS}$ = 1.69 ps. Hence, k_{BET} was calculated as 0.41 ps^{-1}. Hence, band edge electron transfer time; $\tau_{BET} = 1/k_{BET}$ was found as 2.44 ps.

Table S1: Fitting parameters of PL decays for all the systems after 440 nm laser excitation.

	A1 (%)	τ1 (ns)	A2 (%)	τ2 (ns)	A3 (%)	τ3 (ns)	<τ>
P25 TiO_2	28.58	4.13	10.40	17.2	61.02	0.96	10.18
CdS	33.67	3.3	24.29	19.4	42.14	0.61	15.67

TiO_2-CdS	31.20	4.16	22.88	23.03	45.92	0.6	18.54

Table S2. Fitting parameters corresponding to the bleach kinetics for CdS and TiO_2-CdS after 440 nm pump.

	Wavelength (nm)	τ_g (ps)	τ_{d1} (ps)	τ_{d2} (ps)	τ_{d3} (ns)
CdS	500	0.30 (100 %)	1.69 (-17.1%)	28 (-36.6 %)	>1 (-46.3 %)
	590	0.11 (100%)	0.68 (-16.7%)	20.1 (-47.6%)	>1 (-35.7%)
TiO_2-CdS	500	0.1 (100 %)	1 (-23.8%)	17.5 (-38.1%)	>1 (-38.1%)
	590	<0.1 (100 %)	0.25 (-30.2%)	13.5 (-37.2%)	>1 (-32.6%)

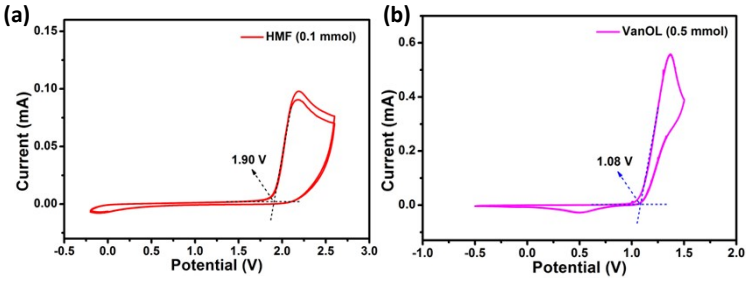

Figure S8. Cyclic voltammetry profiles with oxidation on-set potentials of a) HMF and b) VanOL.

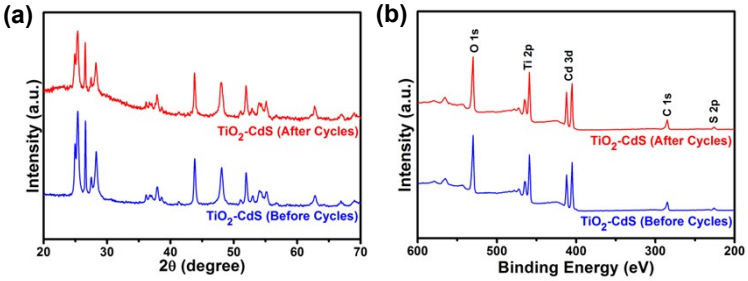

Figure S9. a) Powder XRD patterns; and b) XPS Survey spectra of TiO_2-CdS before and after recyclability.

References

1. J. He, L. Chen, F. Wang, Y. Liu, P. Chen, C. T. Au and S. F. Yin, *ChemSusChem*, 2016, **9**, 624–630.
2. Y. Wang, Z. Hu, W. Wang, H. He, L. Deng, Y. Zhang, J. Huang, N. Zhao, G. Yu and Y.-N. Liu, *Chem. Sci.*, 2021, **12**, 16065.
3. Q. Tan, K. Li, Q. Li, Y. Ding, J. Fan, Z. Xu and K. Lv, *Mater. Today Chem.*, 2022, **26**, 101114.
4. L. G. Devi and R. Shyamala, *Mater. Chem. Front*., 2018, **2**, 796-806.